The Journal of Chemical Physics

Stimulated directional emission induced by two-photon excitation of the Xe 6*p*' and Xe 7*p* states

Cite as: J. Chem. Phys. **146**, 094304 (2017); https://doi.org/10.1063/1.4977522
Submitted: 06 January 2017 . Accepted: 13 February 2017 . Published Online: 03 March 2017

V. A. Alekseev, P. J. M. van der Burgt, and D. W. Setser

Stimulated directional emission induced by two-photon excitation of the Xe 6*p*′ and Xe 7*p* states

V. A. Alekseev,[1,a)] P. J. M. van der Burgt,[2] and D. W. Setser[3]
[1]*St. Petersburg State University, 7/9 Universitetskaya Nab., St. Petersburg 199034, Russia*
[2]*Department of Experimental Physics, National University of Ireland, Maynooth, Co. Kildare, Ireland*
[3]*Department of Chemistry, Kansas State University, Manhattan, Kansas 66506, USA*

(Received 6 January 2017; accepted 13 February 2017; published online 3 March 2017)

Stimulated emission (SE) induced by pulsed two-photon excitation of the $6p'[1/2]_0$, $6p'[3/2]_2$, $7p[1/2]_0$, $7p[3/2]_2$, and $7p[5/2]_2$ states of the Xe atom has been studied. Spectra of SE were recorded in the 800–3500 nm region, which covers the $6p', 7p \rightarrow 7s$ (2500–3500 nm), $6p', 7p \rightarrow 5d$ (1000–2000 nm), $7s \rightarrow 6p$ (1200–1900 nm) transitions, as well as the near-IR $6p \rightarrow 6s$ (800–1000 nm) transitions. It is shown that excitation of the $7p$ states results in radiative cascade via the $7s$ states, $7p \rightarrow 7s \rightarrow 6p$, although at least one case of cascading via the $5d$ states is also observed. Spectra of SE induced by excitation of the $6p'$ states are dominated by the $6p' \rightarrow 6s'$ transitions in the near IR and the $6p' \rightarrow 5d[1/2]_1 \rightarrow 6p[1/2]_1 \rightarrow 6s[3/2]_1$ cascade; the $6p' \rightarrow 7s \rightarrow 6p$ cascade is also observed, although the secondary $7s \rightarrow 6p$ emission is rather weak in comparison with excitation of the $7p$ states. *Published by AIP Publishing.* [http://dx.doi.org/10.1063/1.4977522]

I. INTRODUCTION

Laser excitation of atomic gas near a dipole-allowed two-photon transition creates favorable conditions for the occurrence of various nonlinear optical effects. Typically, one or more excited states of the atom are lying below the two-photon pumped state and are coupled with it by strong dipole allowed transitions. At sufficiently high concentration of the two-photon excited atoms, the light spontaneously emitted along the direction of laser beam (including in the opposite direction) is amplified in the medium. Amplified spontaneous emission (ASE) may cause significant transfer of the population from the laser-pumped state to lower lying states. Two-photon excitation may also induce various parametric processes, including four-wave mixing (FWM), stimulated electronic Raman scattering, and stimulated hyper Raman scattering (see, in particular Ref. 1 and the references cited therein). In contrast to ASE, which requires tuning the laser at the two-photon resonance to create a population inversion, parametric processes occur when the laser frequency is detuned from the two-photon resonance. Another nonlinear process, which commonly accompanies two-photon excitation, is photoionization. This occurs due to the high density of photon flux needed for two-photon excitation. Photoionization is especially efficient when the ionization potential of the two-photon excited state is less than the photon energy, i.e., the exited atom is ionized by absorbing one photon. The presence of photoelectrons at sufficiently high concentrations may significantly influence the nonlinear properties of the gaseous medium.

This study concerns the generation of highly directional emissions in Xe gas induced by two-photon excitation of the Xe $6p'$ and $7p$ states (Xe energy levels diagram is given in Fig. 1). Further in the text, this emission is called stimulated emission (SE) without specifying its nature which could be ASE or Raman or a mixture of both (see below). The first observation of the SE effect in Xe was reported in Ref. 2. Irradiating a cell containing Xe gas at a pressure of 20 Torr with ArF $\lambda = 193$ nm and XeF $\lambda = 351$ nm lasers, the authors observed stimulated $6p[1/2]_0 \rightarrow 6s[3/2]_1$ emission at $\lambda = 828.0$ nm (the combined energy of the $\lambda = 193$ and 351 nm photons matches the $6p[1/2]_0$ energy). In Ref. 2 Xe gas was excited laterally. The length of the volume containing excited Xe atoms was determined by the length of the rectangular laser beams (2.9 cm). In subsequent studies[3,4] the $6p[1/2]_0$ state was excited with the use of tunable frequency doubled radiation of a dye laser propagating along the gas cell axis which provided a longer volume containing excited atoms. Kartazaev[3] reported stimulated emission at 828 nm in the backward direction. Rankin *et al.*[4] recorded the 828 nm emission in both backward and forward directions and observed a linear correlation between emission intensities. Measurements of the ratio of the backward emission energy to the forward one gave a value of 0.4 with a factor of two uncertainty. The maximum intensity was observed when the laser frequency was tuned exactly at the two-photon resonance. The authors concluded that this bidirectional emission most closely corresponded to properties of ASE, although the pressure and power dependences of the signal were somewhat different from theoretical predictions. Their study also reported on the observation of emission propagating at some angle to the laser beam (conical emission) upon detuning the laser frequency by 4–5 GHz to the blue side from the resonance.

The studies discussed above[2–4] were concerned with the low lying $6p[1/2]_0$ two–photon resonant state. A detailed study

a)Author to whom correspondence should be addressed. Electronic mail: alekseev@va3474.spb.edu

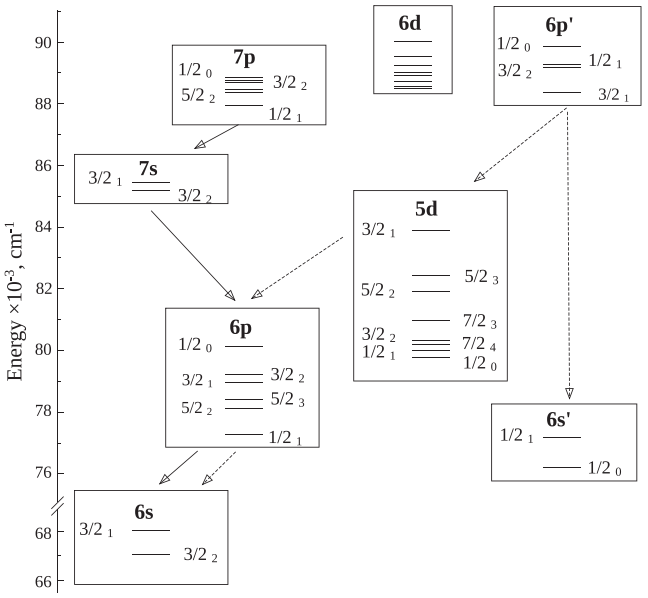

FIG. 1. Diagram of Xe atom levels. States are designated in the *jl*-coupling notation, $nl[K]_J$, where $K = j(5p^5) + l(nl)$, $J = K + 1/2$, and the projection of the angular momentum of the ion core equals to $j(5p^5) = 3/2$ or 1/2; the $j(5p^5) = 1/2$ states are labeled with prime. The $nl[K]_J$ designation of some 7*p* states and all 6d states is omitted because of congestion. The main SE pathways from the 7*p* and 6*p*′ states are shown by solid and dashed arrows, respectively.

of stimulated emission induced by two-photon excitation of higher lying 6*p*′, 7*p* (see Fig. 1), 8p, and 4f states was reported by Miller.[1] Spectra of SE induced by excitation of the 6*p*′ and 7*p* states displayed direct transitions from the laser excited states, 6*p*′, 7*p* → 6*s* in the visible and 6*p*′ → 6*s*′ in the near IR region, as well as 6*p* → 6*s* transitions in the near IR. The number of the 6*p* → 6*s* lines in the spectrum greatly varied for different laser-excited states. For example, in the case of $6p'[1/2]_0$ the spectrum of SE displayed seven 6*p* → 6*s* transitions, whereas only one such transition was observed upon pumping $7p[5/2]_2$.

The presence of the 6*p* → 6*s* lines in the SE spectra is evidence of radiative cascade via 7*s* or 5*d* states acting as intermediates, 6*p*′, 7*p* → 7*s*(5*d*) → 6*p* → 6*s*. These transitions are in the IR region and were not studied in Miller's work because the sensitivity region of the registration system spanned the visible and near IR (up to λ ~ 950 nm). Some of the results obtained by Miller pointed to more complex radiative routes. In particular, SE spectrum following excitation of the $6p'[1/2]_0$ state displayed $6p[5/2]_3 \rightarrow 6s[3/2]_2$ line at 882 nm; as noted by Miller, coupling $6p'[1/2]_0$ with $6p[5/2]_3$ requires a cascade of four transitions via intermediate 6*d*, 7*p*, and 5*d* states, $6p'[1/2]_0 \rightarrow 6d \rightarrow 7p \rightarrow 5d \rightarrow 6p[5/2]_3$.

If the spectral width of the laser is larger than the width of the two-photon resonance, laser excitation can simultaneously induce ASE and parametric Raman emission. Such an effect, in particular, was observed for the $6p[1/2]_0 \rightarrow 6s[3/2]_1$ emission at 828 nm excited by two-photon pumping of the $6p[1/2]_0$ state.[5,6] Experiments showed that the intensity of the 828 nm emission in the forward and backward directions displays different dependencies on laser power and xenon pressure. Excitation spectra of the forward and backward emissions were different too.[6] The excitation spectrum of the forward emission has a larger spectral width and displays a dip at the frequency of the two-photon resonance. The explanation for the different behavior of the forward and backward emissions is that the latter is ASE while the forward emission is a mixture of ASE and parametric emission. In fact, the parametric emission at λ = 828 nm in the forward direction does not lead to population transfer to the $6s[3/2]_1$ state but is accompanied by Vac UV emission in the proximity of the $6s[3/2]_1 \rightarrow 5p^6$ resonance transition at 147 nm. The nonlinear processes of this type, known as parametric (degenerate) FWM, $2h\nu_L \rightarrow h\nu_1 + h\nu_2$, where ν_1 is the frequency of the transition from the two-photon excited state to an intermediate state, and ν_2 is the frequency of the transition from the intermediate state to the ground state, are well studied for alkali metal vapors (for example, Refs. 7–9 reported recent studies of this effect in Rb with the use of various excitation methods). Only a few studies of this parametric effect have been performed in rare gases. Vac UV emission has been reported[10,11] upon excitation of Xe gas by a femtosecond KrF laser. The proximity of this laser wavelength, λ_{KrF} = 248.5 nm, to the wavelength of the $6p[1/2]_0 \leftarrow 5p^6$ two-photon resonance, 249.6 nm, greatly enhances the cross-section of the FWM process. Test experiments aimed at observation of the $6p[1/2]_0 \rightarrow 6s[3/2]_1 \rightarrow 5p^6$ transitions, λ = 828 and 147 nm, respectively, upon pumping Xe $6p[1/2]_0$ were also performed in Ref. 6. These experiments required the use of a vacuum monochromator to separate Vac UV light from the exciting laser emission. Still, strong stray laser light was a complication. It appears likely that excitation of Kr $5p[1/2]_0$ would lead to generation of Kr $(5s[3/2]_1 \rightarrow 4p^6)$ emission at 124 nm. Owing to its simplicity, such a source of Vac UV emission may be of interest for several applications. However, a systematic study is needed for evaluating the conversion efficiency and finding optimal conditions.

Along with the parametric emission, ASE is also of interest for several applications. ASE from two-photon excited states has been proposed and successfully used for the population of atomic states that are otherwise difficult to access optically due to technical reasons or restrictions imposed by selection rules.[6] The ASE method was used to populate the Xe $6s[3/2]_1$,[6,12–14] Xe $6s'[1/2]_1$,[6] Xe $5d[3/2]_1$,[15] and Kr $5s[3/2]_1$[16] resonance states in mixtures with foreign gases for kinetic studies. ASE on the $5p[3/2]_2 \rightarrow 3d[5/2]_3$, $3d[3/2]_2$, and $5s[3/2]_2$ IR transitions in Ar has been suggested (although not observed directly) as an explanation of a fast population transfer following optical excitation to the Ar $5p[3/2]_2$ state from Ar $4s[3/2]_1$; the resonance state was excited in an electric discharge.[17] It is relevant to mention in this context the recently proposed optically pumped rare-gas metastable laser.[18] The population inversion in this device is created by optical excitation of metastable Rg ($ns[3/2]_2$, n = 4, 5, and 6 for Ar, Kr, and Xe, respectively) atoms (generated in an electric discharge) by an array of diode lasers into a higher lying n*p*-state followed by collisional relaxation to the lowest $np[1/2]_1$ level, which decays radiatively to the $ns[3/2]_{1,2}$ states. Another area of applied interest specifically to studies of optical processes induced by two-photon excitation of Xe concerns the use of this gas as a propellant for electric spacecraft thrusters. Two-photon excitation has been used as a technique for diagnostics of the thruster plume plasma.[19]

In this work we report on a study that was mainly aimed at establishing intermediate states involved in the cascading SE effect resulting in $6p \rightarrow 6s$ emission upon excitation of the $6p'$ and $7p$ states. For this purpose, we recorded SE spectra in the 800–3500 nm region, which covers $6p'$, $7p \rightarrow 7s$ (2500–3500 nm), $6p'$, $7p \rightarrow 5d$ (1000–2000 nm), and $7s \rightarrow 6p$ (1200–1900 nm) transitions; the $6p \rightarrow 6s$ transitions in the near IR region (800–1000 nm) were recorded as well. The experiments showed that excitation of $7p$ states results in radiative cascade via the $7s$ states, $7p \rightarrow 7s \rightarrow 6p$, although at least one case of coupling via the $5d$ state was also observed. In turn, the SE spectra upon excitation of the $6p'$ states are dominated by the $6p' \rightarrow 6s'$ transitions in the near IR region and the $6p' \rightarrow 5d[1/2]_1 \rightarrow 6p[1/2]_1 \rightarrow 6s[3/2]_1$ cascade; the $6p' \rightarrow 7s \rightarrow 6p$ cascade is also observed, but the $7s \rightarrow 6p$ lines are rather weak in comparison with excitation of the $7p$ states. Analysis of the spectra showed that in most cases the preference of a given SE cascade over others can be explained on the basis of available *ab initio* data[20] on Einstein coefficients A_{ik} and line strengths S (square of the transition dipole moment).

II. EXPERIMENTAL METHOD

Xe atoms were excited by UV radiation from the frequency-doubled output of a Lambda Physik LPD3002 dye laser pumped by Lambda Physik LEXTRA excimer laser. The excimer laser repetition rate was 10 Hz. Coumarin 120 dye was used to obtain tunable UV radiation in the 222–226 nm region for two-photon excitation of the $6p'$ and $7p$ states. The energy of the UV laser pulses was 0.1–0.5 mJ and the FWHM was about 15 ns. The optical cell was constructed from standard CF65 parts (Leybold) including cross-shape vacuum connectors and CF65 flanges with quartz window and had a length of 25 cm. The pressure in the cell was monitored by a Baratron manometer and a Pirani gauge. Before use the cell and gas handling system was evacuated using a turbomolecular pump. The laser beam was mildly focused using a 50 cm focal length lens. SE co-propagating with the UV laser beam was dispersed by a 0.3 m Acton monochromator and recorded using a PbSe photodiode (Hamamatsu P9696-02). The photodiode signal was digitized by a Tektronix oscilloscope and transferred to a computer using LabVIEW software. Because SE covers a broad spectral region, spectra were recorded using a rather fast scanning speed, which reduced the spectral resolution. The spectra presented in this work have not been corrected for the spectral response of the photodetection system.

III. RESULTS

A. Excitation of the Xe 7*p* states

Study of the SE spectra shows that excitation of the Xe $7p$ states leads to $7p \rightarrow 7s \rightarrow 6p \rightarrow 6s$ cascading SE. The $7p \rightarrow 7s$ transitions are in the 2900–3500 nm region. The SE spectra in this region following excitation of the $7p$ states and the $6p'[3/2]_2$ state are shown in Fig. 2. Assignment of lines is given in Tables I and II.

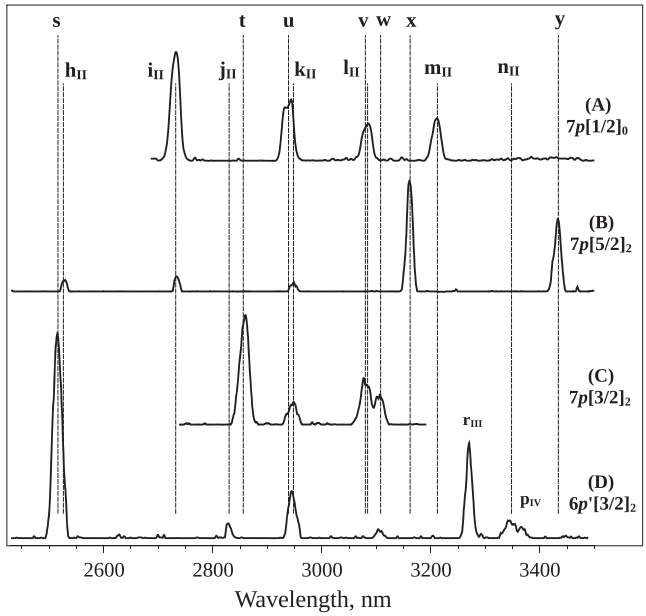

FIG. 2. Spectra of stimulated emission in the 2400–3600 nm region induced by two-photon excitation of the $7p[1/2]_0$, $7p[5/2]_2$, $7p[3/2]_2$, and $6p'[3/2]_2$ states of Xe at P_{Xe} = 115 Torr. The assignment of the transitions is given in Table I. The SE spectrum following excitation of $6p'[1/2]_0$ state at P_{Xe} = 115 Torr was not measured; at P_{Xe} = 270 Torr the spectrum did not have the $6p'[1/2]_2 \rightarrow 7s$ transitions.

Figure 3 shows SE spectra in the 750–1750 nm region following excitation of the three two-photon resonance $7p$-states. The specified region includes the $7s \rightarrow 6p$ transitions (1200–1700 nm) and the $6p \rightarrow 6s$ transitions (800–1000 nm). In terms of the number of $7s \rightarrow 6p$ lines, excitation of $7p[1/2]_0$ gives the simplest spectrum, because this state is coupled only with the $J = 1$ state of the $7s[3/2]_{1,2}$ pair. In turn, $7s[3/2]_1$ is optically coupled with five $6p$ states. Three of these transitions are seen in the SE spectrum (Fig. 3(a), lines labeled **i**, **l**, and **m**). The $7s[3/2]_1 \rightarrow 6p[1/2]_1$ transition at 1224 nm is not observed presumably because of its comparatively weak strength (Table I). Another missing transition is $7s[3/2]_1 \rightarrow 6p[1/2]_0$ at 1879 nm. Its strength is comparable with the strength of transition **m**, which is the weakest among the three observed transitions (Table I) and disappears as the xenon pressure is increased (Fig. 3(a)). One may expect that similar to transition **m**, the $7s[3/2]_1 \rightarrow 6p[1/2]_0$ transition is sensitive to the experimental conditions and may appear at higher excitation energy or optimized Xe pressure.

In addition to the three $7s \rightarrow 6p$ transitions, the spectrum of SE emission following excitation of $7p[1/2]_0$ state (Fig. 3(a)) also shows several $6p \rightarrow 6s$ transitions. This implies occurrence of a cascading $7s[3/2]_1 \rightarrow 6p \rightarrow 6s$ effect. As is seen from Table II, transitions **i** and **m** can be viewed as "precursors" of transitions **f** and **c**, respectively. However, transition **m** completely disappears at increased Xe pressure, whereas transition **c** does not, although its intensity decreases (Fig. 3(a)). A possible explanation of this result is that the upper state of transition **c**, the $6p[3/2]_2$ state, is coupled with the laser pumped $7p[1/2]_0$ state by an alternative route. Considering that the intermediate state should lie below the laser pumped state and be coupled with it, the possible intermediate transitions are

TABLE I. Strongest transitions from $6p'[1/2]_0$, $6p'[3/2]_2$, $7p[1/2]_0$, $7p[3/2]_2$, $7p[5/2]_2$ states and some $5d$ states. Transitions observed in the present work are labeled with letters (see Figs. 2–4). Information about the transitions was taken from Ref. 20.[a] Theoretical results on the transition probabilities were also reported in 21; a comparison of theoretical results of Refs. 20, 21 for the $6p$, $6p'$, and $7p$ states with experimental values was reported in Ref. 22.

Transition		λ (nm)	S, $(a_o e)^2$	A_{ik}, 10^6 s^{-1}	Transition		λ (nm)	S, $(a_o e)^2$	A_{ik}, 10^6 s^{-1}
		$7p[1/2]_0$					$6p'[1/2]_0$		
$7p[1/2]_0 \rightarrow 7s[3/2]_1$	**u**	2939	45.4	3.61	$6p'[1/2]_0 \rightarrow 7s[3/2]_1$		2262.4	8.66	1.51
$7p[1/2]_0 \rightarrow 5d[3/2]_1$		2019	1.99	0.49	$6p'[1/2]_0 \rightarrow 6s'[1/2]_1$	**o**	788.9	5.28	21.70
$7p[1/2]_0 \rightarrow 5d[1/2]_1$	**g ?**	1129	1.93	2.71	$6p'[1/2]_0 \rightarrow 5d[1/2]_1$	**q**	1013	4.2	8.14
$7p[1/2]_0 \rightarrow 6s'[1/2]_1$		858	1.46	4.67	$6p'[1/2]_0 \rightarrow 5d[3/2]_1$		1675	1.53	0.66
$7p[1/2]_0 \rightarrow 6s[3/2]_1$		481	0.281	5.10	$6p'[1/2]_0 \rightarrow 6s[3/2]_1$		458.4	0.144	3.02
		$7p[3/2]_2$					$6p'[3/2]_2$		
$7p[3/2]_2 \rightarrow 7s[3/2]_1$	**v**	3080	111.0	1.54	$6p'[3/2]_2 \rightarrow 7s[3/2]_2$	**s**	2516	26.5	0.67
$7p[3/2]_2 \rightarrow 7s[3/2]_2$	**t**	2859	160.0	2.77	$6p'[3/2]_2 \rightarrow 5d[5/2]_3$		1485	1.21	0.15
$7p[3/2]_2 \rightarrow 5d[5/2]_3$	**m′ ?**	1598	17.3	1.71	$6p'[3/2]_2 \rightarrow 5d[1/2]_1$	**r**	1089	20.5	6.41
$7p[3/2]_2 \rightarrow 5d[1/2]_1$		1149	1.08	0.29	$6p'[3/2]_2 \rightarrow 6s'[1/2]_1$	**p**	835	38.0	26.40
$7p[3/2]_2 \rightarrow 6s'[1/2]_1$		869.4	1.67	1.03	$6p'[3/2]_2 \rightarrow 6s[3/2]_1$		473.6	0.28	1.06
$7p[3/2]_2 \rightarrow 6s[3/2]_1$		484.4	0.21	0.75			$5d \rightarrow 6p$		
$7p[3/2]_2 \rightarrow 6s[3/2]_2$		462.6	1.22	4.98	$5d[3/2]_1 \rightarrow 6p[5/2]_2$		1 733	2.34	0.30
		$7p[5/2]_2$			$5d[3/2]_1 \rightarrow 6p[3/2]_1$		2 027	30.4	2.46
$7p[5/2]_2 \rightarrow 7s[3/2]_1$	**x**	3434	185.0	1.85	$5d[3/2]_1 \rightarrow 6p[1/2]_0$		2 652	35.2	1.27
$7p[5/2]_2 \rightarrow 7s[3/2]_2$	**y**	3162	105.0	1.35	$5d[1/2]_1 \rightarrow 6p[1/2]_1$		3 680	20.6	0.28
$7p[5/2]_2 \rightarrow 5d[7/2]_3$		1355	8.73	1.42	$5d[1/2]_1 \rightarrow 6p[3/2]_2$		1 2917	5.23	0.002
$7p[5/2]_2 \rightarrow 5d[1/2]_1$		1195	2.4	0.57	$5d[7/2]_3 \rightarrow 6p[5/2]_2$		3 508	110	0.74
$7p[5/2]_2 \rightarrow 6s'[1/2]_1$		895.5	1.94	1.09	$5d[7/2]_3 \rightarrow 6p[5/2]_3$		3 895	20.8	0.1
$7p[5/2]_2 \rightarrow 6s[3/2]_1$		492.5	0.17	0.58	$5d[5/2]_3 \rightarrow 6p[5/2]_3$		2 483	25.3	0.48
$7p[5/2]_2 \rightarrow 6s[3/2]_2$		469.8	0.315	12.30	$5d[5/2]_3 \rightarrow 6p[3/2]_2$	**w**	3 108	119	1.14

[a]The values of line strength S (square of transition dipole moment) and Einstein A_{ik} coefficient in this table were calculated in Ref. 20 using the length operator formulation. Ref. 20 also reports results for the same transitions obtained using the velocity operator formulation.

$7p[1/2]_0 \rightarrow 5d[1/2]_1$ and $7p[1/2]_0 \rightarrow 5d[3/2]_1$. These transitions indeed have reasonable strength (Table I). However, the secondary $5d[1/2]_1 \rightarrow 6p[3/2]_2$ and $5d[3/2]_1 \rightarrow 6p[3/2]_2$ transitions, which terminate at the $6p[3/2]_2$ state, are weak. As can be seen from Table I, $5d[1/2]_1 \rightarrow 6p[1/2]_1$ is far stronger and appears preferable for the cascading radiative process. The $6p'[1/2]_0$ (or $6p'[3/2]_2$) $\rightarrow 5d[1/2]_1 \rightarrow 6p[1/2]_1 \rightarrow 6s[3/2]_2$ cascades were indeed observed. In particular, lines **q** and **r** in Figs. 4(d) and 4(e) are transitions from the laser excited state to $5d[1/2]_1$. In contrast, the $7p[1/2]_0 \rightarrow 5d[1/2]_1$ transition is weak (line **g**; see discussion below concerning assignment of this spectral feature). Thus, explanation of the origin of line **c** upon excitation of the $7p[1/2]_0$ state requires additional experiments.

The $7p[3/2]_2$ and $7p[5/2]_2$ states are coupled with both $7s[3/2]_1$ and $7s[3/2]_2$ states. The corresponding transitions have comparable strength and both are present in the spectra: lines **t** and **v** in Fig. 2(c) and lines **x** and **y** in Fig. 2(b). In the **t/v** and **x/y** pairs the short wavelength line is more intense. This result may be explained on the basis of line strength values: as is seen from Table II, the short wavelength transitions are stronger both in terms of the Einstein A_{ik} coefficient and the line strength S (or, in fact, the Einstein B_{ik} coefficient for stimulated emission, which, similar to A_{ik} coefficient, is

TABLE II. The strongest $7s \rightarrow 6p \rightarrow 6s$ transitions. Information about the transitions was taken from Ref. 20 (see footnotes to Table I). Lines observed in the present work are labeled with letters (see Figs. 2–4).

		$7s \rightarrow 6p$					$6p \rightarrow 6s$		
Transition		λ (nm)	S, $(a_o e)^2$	A_{ik}, 10^6 s^{-1}	Transition		λ (nm)	S, $(a_o e)^2$	A_{ik}, 10^6 s^{-1}
$7s[3/2]_1 \rightarrow 6p[1/2]_1$		1224	1.5	0.54	$6p[1/2]_1 \rightarrow 6s[3/2]_1$		1084.1	4.9	2.61
$7s[3/2]_2 \rightarrow 6p[1/2]_1$	**h**	1263	22.5	4.54	$6p[1/2]_1 \rightarrow 6s[3/2]_2$	**e**	980	43.3	31.0
$7s[3/2]_1 \rightarrow 6p[5/2]_2$	**i**	1366	31.5	8.34	$6p[5/2]_2 \rightarrow 6s[3/2]_1$	**f**	993	47.3	19.6
$7s[3/2]_2 \rightarrow 6p[5/2]_2$	**j**	1415	16.2	2.31	$6p[5/2]_2 \rightarrow 6s[3/2]_2$		905	19.6	10.7
$7s[3/2]_2 \rightarrow 6p[5/2]_3$	**k**	1474	73.8	9.35	$6p[5/2]_3 \rightarrow 6s[3/2]_2$	**b**	882	93.0	39.2
$7s[3/2]_1 \rightarrow 6p[3/2]_1$	**l**	1542	31.2	5.74	$6p[3/2]_1 \rightarrow 6s[3/2]_1$	**d**	917	36.0	31.6
$7s[3/2]_2 \rightarrow 6p[3/2]_1$		1604	2.5	0.24	$6p[3/2]_1 \rightarrow 6s[3/2]_2$		841.2	1.62	18.4
$7s[3/2]_1 \rightarrow 6p[3/2]_2$	**m**	1606	19.9	3.24	$6p[3/2]_2 \rightarrow 6s[3/2]_1$	**c**	895	18.8	10.6
$7s[3/2]_2 \rightarrow 6p[3/2]_2$	**n**	1673	43.6	3.77	$6p[3/2]_2 \rightarrow 6s[3/2]_2$	**a**	823	34.2	24.9
$7s[3/2]_1 \rightarrow 6p[1/2]_0$		1879	16.1	1.64	$6p[1/2]_0 \rightarrow 6s[3/2]_1$		828.2	12.5	44.5

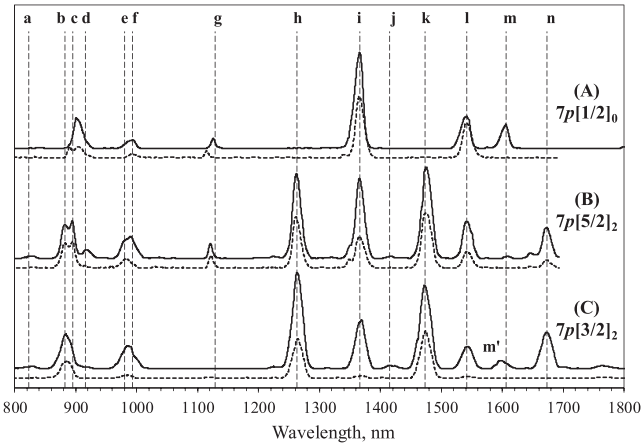

FIG. 3. Spectra of stimulated emission following two-photon excitation of Xe $7p[1/2]_0$, Xe $7p[5/2]_2$, and Xe $7p[3/2]_2$ states. Solid line—P_{Xe} = 115 Torr, dashed line—P_{Xe} = 270 Torr. The assignment of the transitions is given in Tables I and II Spectra are not corrected for the spectral response function of the registration system.

proportional to the line strength but does not depend on the transition wavelength).

In addition to the $7p \rightarrow 7s$ transitions, the spectrum in Fig. 2(c) displays an extra line assigned to the $5d[5/2]_3 \rightarrow 6p[3/2]_2$ transition (line **w**). The presence of this transition points to a cascading effect. The parent $7p[3/2]_2 \rightarrow 5d[5/2]_3$ transition at 1598 nm is rather strong (Table I). As is seen from Fig. 3(c), the SE spectrum indeed shows a line labeled **m′** that matches the wavelength of this transition. Due to the insufficient resolution and closeness to the $7s[3/2]_1 \rightarrow 6p[3/2]_2$ transition at 1606 nm (line **m**), the assignment of line **m′** is tentative.

Relative to the SE spectrum following excitation of $7p[1/2]_0$ (Fig. 3(a)), the spectra corresponding to excitation of $7p[5/2]_2$ and $7p[3/2]_2$ (Figs. 3(b) and 3(c)) display additional lines labeled **h**, **k**, and **n** corresponding to the three strongest transitions from $7s[3/2]_2$ (Table II). The results of our experiments indicate that variation of the Xe pressure has a stronger effect on the $7s[3/2]_1 \rightarrow 6p$ lines in comparison with the $7s[3/2]_2 \rightarrow 6p$ lines. For instance, in the case of excitation of $7p[3/2]_2$, the $7s[3/2]_1 \rightarrow 6p$ lines completely disappear as Xe pressure increases (Fig. 3(c)). A likely explanation is "switching-off" the parent $7p[3/2]_2 \rightarrow 7s[3/2]_1$ transition (line **v** in Fig. 2(c)), which is weaker than the $7p[3/2]_2 \rightarrow 7s[3/2]_2$ transition (line **t**). At conditions well above the threshold of the $7p \rightarrow 7s$ SE, the pressure dependence of secondary $7s \rightarrow 6p$ lines can be distinct for each individual transition determined by its radiative characteristics. Examples of pressure and power dependences for several transitions in the SE spectra are given in Ref. 5. No measurements of this kind were performed in the course of this work. As noted in the Introduction, spectrographs allowing simultaneous observation of several lines are better suited for such a study.

Concluding this section, we discuss the feature labeled **g** in Figs. 3(a) and 3(b). This feature is in close proximity to the $7p[1/2]_0 \rightarrow 5d[1/2]_1$ transition. When the $7p[1/2]_0$ state is pumped, the presence of this transition in the SE spectrum might have a natural explanation considering its significant line strength and rather large A_{ik} coefficient, although the spectrum shows no $7p[1/2]_0 \rightarrow 6s'[1/2]_1$ transition, which is characterized by a comparable line strength and a significantly larger A_{ik} coefficient (Table I). However, it should be also noted that in one of the two spectra shown in Fig. 3(a) this line is significantly shifted from the position of the $7p[1/2]_0 \rightarrow 5d[1/2]_1$ transition. Furthermore, the spectrum following excitation of $7p[5/2]_2$ also shows a line in this region. Although $7p[1/2]_0$ and $7p[5/2]_2$ are coupled optically via close-lying $6d$ states, cascading radiative effect involving $7p[1/2]_0$ is prohibited because the laser pumped $7p[5/2]_2$ state lies 490 cm^{-1} below. The origin of line **g** cannot be unambiguously explained on the basis of available experimental data and is one of the questions addressed to further studies.

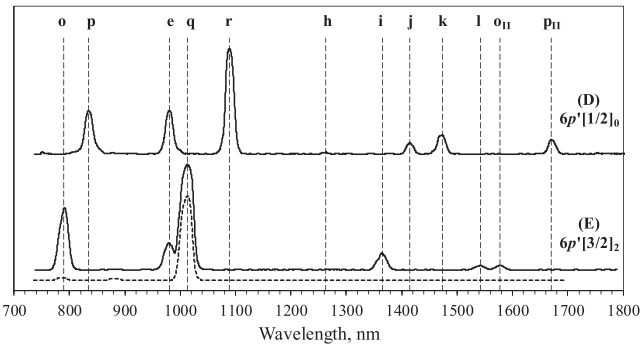

FIG. 4. Spectra of stimulated emission following two-photon excitation of Xe $6p'[1/2]_0$ and Xe $6p'[3/2]_2$. Solid line—P_{Xe} = 115 Torr, dashed line—P_{Xe} = 270 Torr. The assignment of the transitions is given in Tables I and II Spectra are not corrected for the spectral response function of the registration system.

B. Excitation of the 6p′ states

The spectra of stimulated emission following excitation of the $6p'$ states show a different intensity distribution pattern in comparison with the $7p$ states. As is seen from Fig. 4, excitation of the $6p'[1/2]_0$ and $6p'[3/2]_2$ states yields strong SE to the $6s'[1/2]_1$ state (lines **o** and **p**). Yet another feature for both states is the presence of a strong transition from the laser-pumped state to the $5d[1/2]_1$ state (lines **q** and **r** in Fig. 4) and the $6p[1/2]_1 \rightarrow 6s[3/2]_2$ transition (line **e**). The latter points to the $6p' \rightarrow 5d[1/2]_1 \rightarrow 6p[1/2]_1 \rightarrow 6s[3/2]_2$ cascade. As is seen from the data presented in Tables I and II, all transitions involved in this cascade are characterized by large values of S and A_{ik}. This mechanism was confirmed by recording the $5d[1/2]_1 \rightarrow 6p[1/2]_1$ transition at 3680 nm (spectrum not shown).

Similar to the $7p$ states, excitation of the $6p'$ states results in SE to the $7s$ states. This is illustrated by the spectrum in Fig. 2(d) showing the $6p'[3/2]_2 \rightarrow 7s[3/2]_2$ transition (line **s**). However, the secondary $7s \rightarrow 6p$ lines in the 1200–1800 nm region (Fig. 4) are weak in comparison with the $6p' \rightarrow 6s'$ and $6p' \rightarrow 5d[1/2]_1$ lines. The result can be readily explained considering that the latter transitions are significantly stronger than the $6p' \rightarrow 7s$ transitions (Table I). Also, the SE spectra in Fig. 4 show no secondary $6p \rightarrow 6s$ transitions in the 800–1000 nm region, indicating that the threshold condition for the last transition in the $6p' \rightarrow 7s \rightarrow 6p \rightarrow 6s$ cascade

is not fulfilled. It should be noted in this respect that several lines corresponding to the $6p \rightarrow 6s$ transitions, including lines **a**–**d**, were observed following excitation of the $6p'$ states in Ref. 1. It cannot be excluded, however, that the $6p$ states couple with the $6p'$ states via $5d$ states and not via the $7s$ states.

Concluding this section, we note another interesting observation. Figure 4(e) shows SE spectra recorded at two Xe pressures. As seen, lines **e**, **i**, and **l** corresponding to the secondary transitions disappear at high Xe pressure indicating that the threshold conditions for these transitions or preceding transitions in SE cascade are not fulfilled. However, a less expected result is the absence of line **o** corresponding to the direct $6p'[1/2]_0 \rightarrow 6s'[1/2]_1$ transition because this transition is stronger than $6p'[1/2]_0 \rightarrow 5d[1/2]_1$ (line **q**) both in terms of S and A_{ik} (Table I). It should be noted in this respect that if SE is triggered by spontaneously emitted photons, then for a pair of transitions with comparable line strength, the transition with a larger A_{ik} coefficient is expected to have a lower threshold because SE is triggered by spontaneously emitted photons. However, the discussed result obviously contradicts this simplified picture.

IV. DISCUSSION

A detailed study of stimulated emission following two-photon excitation of Xe was reported by Miller.[1] In comparison with Miller's work, we observed less secondary $6p \rightarrow 6s$ transitions. One reason is the limited spectral resolution of our study, not allowing an unambiguous assignment of some transitions in the SE spectra. In particular, this concerns the close lying $6p[3/2]_2 \rightarrow 6s[3/2]_1$ and $6p[3/2]_1 \rightarrow 6s[3/2]_1$ transitions, which are overlapped in our spectra (lines **c** and **d** in Fig. 3) but were resolved in study.[1] It also cannot be excluded that some of the lines observed by Miller were not observed in the present work due to their weakness combined with the large spectral width associated with the poor resolution. However, in most cases the larger number of the secondary $6p \rightarrow 6s$ lines in the SE spectra reported by Miller most likely is determined by the threshold condition. For instance, in the case of excitation of the $6p'[1/2]_0$ state, we observed no $6p \rightarrow 6s$ transitions in the 820–950 nm region, whereas seven (!) such transitions were observed in Ref. 1 including the three transitions observed upon excitation of the $7p[1/2]_0$ state. The latter result is discussed in some detail below.

Besides the $6p[3/2]_2 \rightarrow 6s[3/2]_1$ and $6p[3/2]_1 \rightarrow 6s[3/2]_1$ transitions (**c** and **d** in Fig. 3), exciting the $7p[1/2]_0$ state Miller also observed the $6p[3/2]_1 \rightarrow 6s[3/2]_2$ transition at 841 nm, but no $6p[1/2]_0 \rightarrow 6s[3/2]_1$ transition at 828 nm, which is characterized by significantly larger values of S and A_{ik} (Table II). This indicates that the threshold condition is not fulfilled either for the second or third step of the $7p[1/2]_0 \rightarrow 7s[3/2]_1 \rightarrow 6p[1/2]_0 \rightarrow 6s[3/2]_1$ cascade. Interestingly, the 828 nm transition was among the seven lines observed in Ref. 1 upon excitation of $6p'[1/2]_0$. It appears unlikely that the threshold condition is fulfilled for all steps of the $6p'[1/2]_0 \rightarrow 7s[3/2]_1 \rightarrow 6p[1/2]_0 \rightarrow 6s[3/2]_1$ cascade upon excitation of $6p'[1/2]_0$ but not fulfilled when the $7p[1/2]_0$ state was excited. Indeed, as shown in the present study, the dominant pathway in the former case involves the $6p'[1/2]_0 \rightarrow 5d[1/2]_1$ transition, whereas it is the $7p[1/2]_0 \rightarrow 7s[3/2]_1$ transition in the latter case. However, $5d[1/2]_1$ lies below $6p[1/2]_0$ and cannot be an intermediate step for a cascade terminating by $6p[1/2]_0 \rightarrow 6s[3/2]_1$. A likely candidate is the $5d[3/2]_1$ state: both transitions in the $6p'[1/2]_0 \rightarrow 5d[3/2]_1 \rightarrow 6p[1/2]_0$ cascade are strong in terms of S and A_{ik} (Tables I and II). On the other hand, upon excitation of the $6p'[1/2]_0$ state Miller also observed the $6p[5/2]_3 \rightarrow 6s[3/2]_2$ transition at 882 nm (labeled **b** in Fig. 3(a)). As noted by the author, coupling $6p'[1/2]_0$ with $6p[5/2]_3$ requires a cascade of four transitions $6p'[1/2]_0 \rightarrow 6d \rightarrow 7p \rightarrow 5d \rightarrow 6p[5/2]_3$. It cannot be excluded that the presence of the $6p[1/2]_0 \rightarrow 6s[3/2]_1$ line is also the result of a more complex mechanism.

Stimulated emission is very sensitive to the experimental conditions, which is not surprising for a nonlinear phenomenon with threshold-type dependence on the experimental conditions. It is interesting to note in this respect that, although we observed fewer secondary $6p \rightarrow 6s$ lines than in Miller's study, the experimental conditions including the energy of exciting laser pulse, Xe pressure, cell length, and focal distance of the lens were similar (even the laser systems were from the same manufacturer). Obviously SE is sensitive to such parameters as detuning from the two-photon resonance, the spectral width of the laser emission, and other characteristics of the laser that are determined by its alignment.

Concluding this section, we note that the intensity of SE seems to be much less influenced by the quenching of the laser excited $7p$ and $6p'$ atoms by collisions with Xe than would be expected considering that the quenching rate constants of the $7p$ and $6p'$ states by Xe are in the region of $k_q \sim (4–5)\ 10^{-10}$ cm^3/s.[5,22] The spectra in Figs. 2–4 were recorded at $P_{Xe} = 115$ and 270 Torr; and the corresponding quenching rate, k_q [Xe] $\sim (1–2)\ 10^9\ s^{-1}$, is much larger than the spontaneous radiative decay rate of the $6p'$ and $7p$ states (radiative lifetime of the $6p'$ states is $\sim 35 \pm 5$ ns and ~70–130 ns for the $7p$ states, see Refs. 5 and 22 and the references therein). One may think that the decrease in the concentration of the excited atoms due to quenching is compensated by the increase in the excitation rate, which is also proportional to the concentration of the ground state atoms, k_{ex} [Xe], where k_{ex} is the coefficient characterizing two-photon absorption at a given laser power (and other experimental conditions except Xe pressure). However, as shown in Ref. 6 adding up to 20 Torr of gases such as CH_4, N_2O, and SF_6 has little effect on the SE intensity. Quenching rate constants of the $6p'$ and $7p$ states by these molecules are in the range of $k_q \sim (2–4)\ 10^{-9}$ cm^3/s and, thus, at P ~ 20 Torr the quenching rate is comparable with that at few hundred Torr of Xe.

The influence of gas pressure on SE signals is expected to be less for Raman type processes than for ASE, because the latter requires the accumulation of enough excited atoms to reach the threshold concentration. It should be noted in this respect that experiments performed in Ref. 6 showed that the cascade $6p \rightarrow 6s$ emission induced by excitation of the $6p'$ and $7p$ states propagates only in the forward direction. Although not conclusive, the available experimental results

suggest that the cascade SE is probably a parametric Raman emission.

V. CONCLUSIONS

The main aim of the present study was to establish the intermediates involved in the cascading SE effects that give the $6p \rightarrow 6s$ lines. Experiments showed that excitation of $7p$ states results in radiative cascade via the $7s$ states, $7p \rightarrow 7s \rightarrow 6p$, although at least one case of coupling via the $5d$ state, $7p[3/2]_2 \rightarrow 5d[5/2]_3 \rightarrow 6p[3/2]_2$, was also observed. In turn, the SE spectra upon excitation of the $6p'$ states are dominated by the $6p' \rightarrow 6s'$ transitions and $6p' \rightarrow 5d[1/2]_1 \rightarrow 6p[1/2]_1 \rightarrow 6s[3/2]_1$ cascade; the $6p' \rightarrow 7s \rightarrow 6p$ cascade is also observed but the $7s \rightarrow 6p$ lines are rather weak relative to excitation of the $7p$ states.

The present study answered several questions, but also raised new questions. One question concerns the role of the line strength and the A_{ik} coefficient in triggering SE. For at least one example, a transition characterized by smaller values of S and A_{ik} has a lower threshold than a transition having larger values of these parameters. Another question concerns the role of experimental conditions. Although we observed far less secondary $6p \rightarrow 6s$ lines than in Miller's study,[1] such "macroscopic" experimental conditions as the energy of exciting laser pulse, Xe pressure, cell length, and focal distance of the focusing lens were similar. Apparently some other experimental parameters, perhaps including the spectral width of the exciting laser radiation and the value of detuning from the two-photon resonance, play a key role in fulfillment of the threshold conditions of the SE effect.

Stimulated emission induced by two-photon excitation of high lying states of Xe atom with its variety of competing radiative decay channels from a given laser pumped state including cascading IR emission is an interesting system for further study. In the present study we used a scanning monochromator to record the SE spectra. Measurements in a broad spectral region using a monochromator are time demanding and, what is more important, experimental conditions may change during the scan (small changes in the laser wavelength and alignment of doubling crystal due to vibrations and heating of equipment during operation, etc). For these reasons, dependences of the SE on the pressure and laser power were not measured. A systematic study of the power and pressure dependences for various lines in the SE spectra would require an experimental setup equipped with several spectrographs enabling simultaneous recording in a broad spectral region from the visible ($7p$, $6p' \rightarrow 6s$ transitions) to IR ($7p$, $6p' \rightarrow 5d$ transitions). Recording emission in the backward and forward direction would allow distinguishing ASE from parametric Raman emission. It should be also noted that because Xe has nine stable isotopes including two isotopes, ^{129}Xe and ^{131}Xe, with nonzero nuclear momentum, the structure of an optical transition in Xe is rather complex and includes single lines of seven isotopes with zero nuclear momentum and lines corresponding to transitions between hyperfine levels of ^{129}Xe and ^{131}Xe. The total bandwidth, which spans a region of several GHz (an example of the hyperfine structure of an Xe line is given in Ref. 23), is less than the width of a dye laser operating without etalon (~20 GHz) and, therefore, all nine isotopes are excited. Nonetheless, the rich hyperfine structure of Xe transitions may complicate studies of nonlinear effects. In particular, due to the different abundances, ASE threshold for different isotopes is reached at different pressures of Xe gas consisting of a mixture of stable isotopes; in turn, in the case of excitation of the Raman emission, the detuning from the two-photon resonance at a given laser wavelength is different for different hyperfine structure transitions. The influence of these effects weakens when the spectral width of the pressure-broadened ASE emission or, in the case of excitation of the Raman emission, detuning the laser frequency from the resonance is significantly larger than the characteristic width of the hyperfine structure.

ACKNOWLEDGMENTS

Dr. Marcin Gradziel is acknowledged for help with data acquisition software. The experiments reported in this paper were performed in 2009. V.A. thanks Science Foundation of Ireland for support via a Walton Visitor Award (No. 07/W.1/I1819).

[1] J. C. Miller, Phys. Rev. A **40**, 6969 (1989).
[2] A. W. McCown, M. N. Edinger, and J. G. Eden, Phys. Rev. A **26**, 2281 (1982).
[3] V. A. Kartazaev, Opt. Spectrosc. **62**, 425 (1987).
[4] M. B. Rankin, J. P. Davis, C. Giranda, and L. C. Bobb, Opt. Commun. **70**, 345 (1989).
[5] V. A. Alekseev and D. W. Setser, J. Phys. Chem. **100**, 5766 (1996).
[6] V. A. Alekseev and D. W. Setser, J. Chem. Phys. **105**, 4613 (1996).
[7] E. Brekke and L. Alderson, Opt. Lett. **38**, 2147 (2013).
[8] A. Akulshin, Ch. Perrella, G.-W. Truong, R. McLean, and A. Luiten, J. Phys. B: At., Mol. Opt. Phys. **45**, 245503 (2012).
[9] C. V. Sulham, G. A. Pitz, and G. P. Perram, Appl. Phys. B **101**, 57 (2010).
[10] A. Tünnermann, K. Mossavi, and B. Wellegehausen, Phys. Rev. A **46**, 2707 (1992).
[11] S. P. Le Blanc, Z. Qi, and R. Sauerbrey, Appl. Phys. B **61**, 439 (1995).
[12] H. Umemoto, Phys. Chem. Chem. Phys. **5**, 5392 (2003).
[13] H. Umemoto, J. Chem. Phys. **125**, 034306 (2006).
[14] H. Umemoto, J. Chem. Phys. **127**, 014304 (2007).
[15] V. A. Alekseev and D. W. Setser, J. Phys. Chem. A **103**, 8396 (1999).
[16] V. A. Alekseev and D. W. Setser, J. Phys. Chem. A **103**, 4016 (1999).
[17] E. Carbone, E. van Veldhuizen, G. Kroesen, and N. Sadeghi, J. Phys. D: Appl. Phys. **48**, 425201 (2015).
[18] J. Han and M. C. Heaven, Opt. Lett. **37**, 2157 (2012).
[19] Ch. Eichhorn, S. Fritzsche, S. Löhle, A. Knapp, and M. Auweter-Kurtz, Phys. Rev. E **80**, 026401 (2009).
[20] M. Aymar and M. Coulombe, At. Data Nucl. Data Tables **21**, 537 (1978).
[21] A. V. Loginov and P. F. Gruzdev, Opt. Spectrosc. **41**, 104 (1976).
[22] M. R. Bruce, W. B. Layne, C. A. Whitehead, and J. W. Keto, J. Chem. Phys. **92**, 2917 (1990).
[23] D. Zhong and D. W. Setser, Chem. Phys. Lett. **207**, 555 (1993).